High-speed imaging system to visualize particle removal/collection via wipe sampling and aerodynamic sampling

Matthew Staymates, Greg Gillen and Jessica Staymates

View Online

Export Citation

CrossMark

ARTICLES YOU MAY BE INTERESTED IN

Flow visualization of an N95 respirator with and without an exhalation valve using schlieren imaging and light scattering
Physics of Fluids **32**, 111703 (2020); https://doi.org/10.1063/5.0031996

Cryogen-free variable temperature scanning SQUID microscope
Review of Scientific Instruments **90**, 063705 (2019); https://doi.org/10.1063/1.5085008

The production of monodisperse explosive particles with piezo-electric inkjet printing technology
Review of Scientific Instruments **86**, 125114 (2015); https://doi.org/10.1063/1.4938486

Nanopositioning Systems

Modular Motion Control

AFM and NSOM Instruments

Single Molecule Microscopes

MAD CITY LABS INC.
www.madcitylabs.com

High-speed imaging system to visualize particle removal/collection via wipe sampling and aerodynamic sampling

View Online   Export Citation   CrossMark

Matthew Staymates,[a) Greg Gillen, and Jessica Staymates

AFFILIATIONS

Material Measurement Laboratory, National Institute of Standards and Technology, 100 Bureau Drive, Gaithersburg, Maryland 301-975-3913, USA

a)Matthew.staymates@nist.gov

ABSTRACT

This work describes a high-speed imaging system that enables the microscopic visualization of the removal and collection of micrometer-sized particles from surfaces during wipe sampling and aerodynamic sampling events. The system features a high-speed digital camera, microlens, custom sample mount and sampling sled, and an illumination source. This imaging system enables direct visualization of wipe-particle and particle-particle interactions during sampling and provides insights relevant to the dynamics of particle removal and collection. Examples of common and adhesive-modified wipe materials sampling polymer microspheres and an explosive-laden fingerprint are given, along with visualization of particle removal via air jet impingement.

INTRODUCTION

Wipe sampling of surfaces for collection of particulates is a critical component in environmental, physical and homeland security, and forensic related applications. Of particular interest to the current study is the optimization of trace contraband detection systems (explosives and narcotics) that rely on wipe-based sampling at security checkpoints.[1–7] Another sampling technique is aerodynamic sampling, a noncontact approach to collecting material from surfaces that relies on fluid dynamics to liberate and transport particulates.[8–10] While the canine is a highly sophisticated example of sampling detection from nature,[11,12] manmade examples include physical screening of both people[13,14] and belongings.[15]

Wipe sampling is typically performed by a human operator and is thus prone to a high level of variability in collection efficiency.[16–18] Several groups have addressed this variability by trying to improve the collection efficiency of the wiping material or better training of the operator. These efforts include the addition of an adhesive material,[19] modification of the surface chemistry,[20] intentionally aging wipes,[21,22] the use of force sensing elements.[17,23] To understand the variations in particle collection efficiency under different

experimental conditions, the imaging system reported here was developed to visualize how particles and surface residues are interacting with the substrate and the swab or air jet during the sampling event and can be used to help explain measured particle collection efficiencies and sources of variations. Additionally, this instrument may help elucidate fundamental particle release mechanisms during air jet impingement that could improve particle removal efficiency for next-generation aerodynamic sampling systems.

SYSTEM DESCRIPTION

The imaging system, shown in Fig. 1, features a high-speed digital camera (APX-RS, Photron.com), microlens (Zoom 6000 series, Navitar.com), a custom sample mount and sampling sled, and a fiber optic illumination source (MLC-150C, Motic.com). The sample mount holds a standard 25 mm × 75 mm glass microscope slide upon which the particles of interest are placed. The end of the lens contains a mirror positioned 45° from horizontal and places the camera viewpoint underneath the glass microscope slide. For swipe-based visualization experiments, a custom 3D-printed sampling sled[24] is used to hold the wipe material, and steel weights are
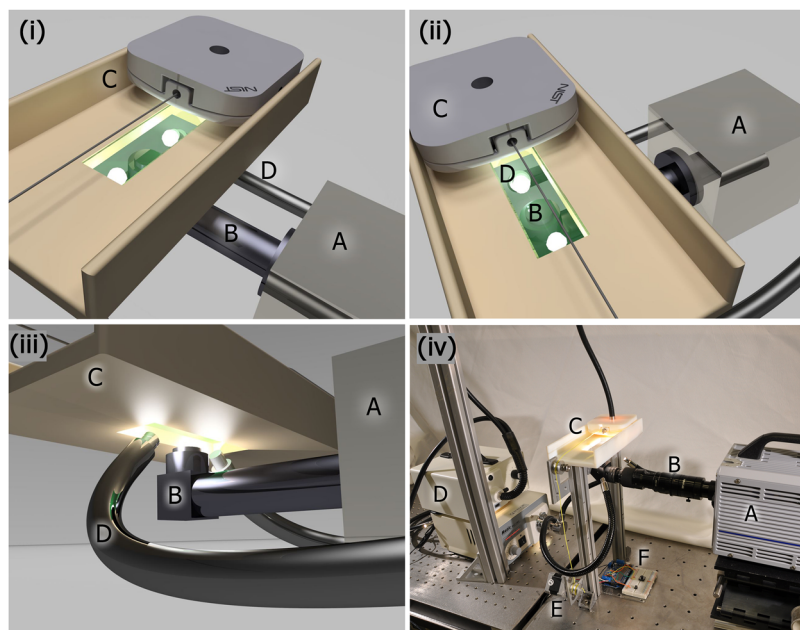
FIG. 1. High-speed imaging system for visualizing particle collection via wipe sampling. Parts (i)–(iii) are 3D computer aided design (CAD) renderings of the system, and (iv) is a photograph of the entire instrument. In each image, (A) represents the high-speed camera, (B) is the lens system, (C) is the sampling sled/U-shaped channel, (D) is the fiber optic illumination source, (E) is the stepper motor used to pull the sled, and (F) is the stepper motor controller.

added to the sled to control the force applied during wiping. The sled rests in a U-shaped channel that restricts the motion of the sled to one direction. The glass slide is positioned in a rectangular recess in the bottom of the channel such that the glass is level with the channel floor. During a swiping event, the sampling sled is pulled across the glass slide while the camera is recording. This allows the operator to look through the glass at the interaction between glass, particles being removed, and a wipe material moving across the screen.

The high-speed camera used here can produce full resolution images (1024 pixels × 1024 pixels) at up to 3000 frames per second (FPS). The image magnification is variable, allowing for a frame size that ranges between 11 mm × 11 mm (92 pixels/mm) to 1.6 mm × 1.6 mm (637 pixels/mm). This results in the ability to visualize particles with diameters on the order of tens of micrometers.

The sampling sled is translated across the glass substrate with a stepper motor, flywheel, and wire. The wire is attached to the sled which is pulled as the motor winds the wire around the flywheel. We use an Arduino microcontroller and stepper motor controller (arduino.cc) for motion control.

For aerodynamic sampling visualization experiments, no swiping sled is required. Instead, an air jet nozzle is positioned above the substrate at a fixed angle and standoff distance. The high-speed camera must be operated at a relatively fast camera image acquisition speed, usually around 50 000 FPS, to capture the rapid events that occur during air jet impingement.

EXAMPLES OF WIPE SAMPLING VISUALIZATION

Several example videos showing typical results from this measurement system are given here. Each of the subsequent figures represents the first frame in a video and has an associated multimedia video file link. In each example, the sled is moving at 65 mm/s,

and the camera is recording at 1000 FPS. The applied force during wiping is governed by the mass of the sampling sled and was measured to be 2 Newtons using a balance.

Figure 2 (Multimedia view) shows five examples of swipe sampling visualization. The first two [(a) and (b)] show Teflon-coated fiberglass (TCF) swabs with and without adhesive, and the second two [(c) and (d)] show a paper-based swab material with and without adhesive, all sampling 39 μm diameter polystyrene latex (PSL) microspheres. These commercially available swab materials are commonly used for trace chemical detection because of their low chemical background, robustness, and resistance to high temperatures. PSL microspheres were used because they are monodisperse and easy to visualize for these initial experiments. The PSL microspheres were dry-deposited onto the glass microscope slide substrate by tapping the PSL container lid on the glass. Figure 2(e) (Multimedia view) shows a Teflon-coated woven fiberglass wipe sampling composition C4 explosive material on a glass slide. C4 is a complex granular material that contains solid RDX particles embedded in a non-Newtonian binder.[25] The sample is prepared by contaminating a gloved thumb with C4 and then making a single thumbprint onto a glass slide. This sample represents real explosive particles that are under investigation during screening.

The videos provide some interesting insights into the dynamics of particle collection using these swipes. The peak and valley surface topography of this TCF swab is clear. In Fig. 2(a) (Multimedia view), direct contact and particle collection only occurs at the "peaks" on the swab surface. Minimal contact is made in the valleys of the swab, resulting in a "channeling" of particles into areas between peaks that may help explain the relatively poor collection efficiency of this particular swab material.[19] Another observation is a "billiard ball" effect where particles are observed to collide with a cluster of other particles and assist in the removal process. By contrast, there is a
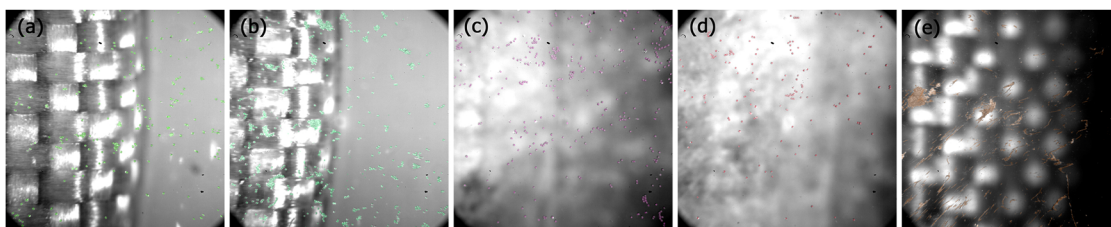
FIG. 2. (a) Regular TCF swab. (b) Adhesive TCF swab sampling PSL microspheres. The swab is moving from left to right and is partially visible in these images. (c) Regular paper-based swab and (d) adhesive paper-based swab sampling PSL microspheres. The swab is moving from left to right and is partially visible in this image. The PSLs have been artificially colored for clarity and are randomly distributed. (e) shows a TCF swab sampling a C4 fingerprint. Multimedia views: (a) https://doi.org/10.1063/1.5096488.1; (b) https://doi.org/10.1063/1.5096488.2; (c) https://doi.org/10.1063/1.5096488.3; (d) https://doi.org/10.1063/1.5096488.4; (e) https://doi.org/10.1063/1.5096488.5

"snow-plow" effect that occurs as the swab contacts the glass substrate in Fig. 2(b) (Multimedia view). The adhesive-coated sampling swab collects all the PSLs within several millimeters after the swab contacts the surface.

The paper-based swab material does not have the uniform weave structure shown in the previous example; rather it consists of pressed paper fibers in random orientations. In Fig. 2(c) (Multimedia view), no apparent snow-plowing occurs, but it does eventually collect most of the PSLs in the field-of-view. In Fig. 2(d) (Multimedia view), the snow-plow effect is obvious when the swab makes contact with the glass surface. Almost all the PSLs are removed immediately upon contact, again demonstrating the different particle collection mechanisms occurring with adhesive vs nonadhesive swabs.

In Fig. 2(e) (Multimedia view), the peak and valley pattern of the woven fiberglass plays a significant role in how material is collected from the substrate. The peaks do much of the collection, while the valleys serve to channel material into a linear pattern. At least qualitatively, larger particles appear to be collected more than the smaller particles and agrees with other work suggesting the dependence between particle collection and size.[26]

EXAMPLES OF AERODYNAMIC SAMPLING VISUALIZATION

An example of aerodynamic sampling visualization is shown in Fig. 3 (Multimedia view). Polymer microspheres (39 μm diameter) are deposited onto a glass slide by dry deposition [Fig. 3 (Multimedia view), left] or with sebaceous fingerprint material [Fig. 3 (Multimedia view), right] by touching the particles with a finger and pressing onto the slide. A single 500 ms jet pulse at 413 kPa, 45° from horizontal, a standoff distance of 50 mm, and a nozzle exit diameter of 1 mm was used. Jet flow is from the upper right to lower left of the frame. The camera was filming at 50 000 FPS at a resolution of 256 pixels × 128 pixels.
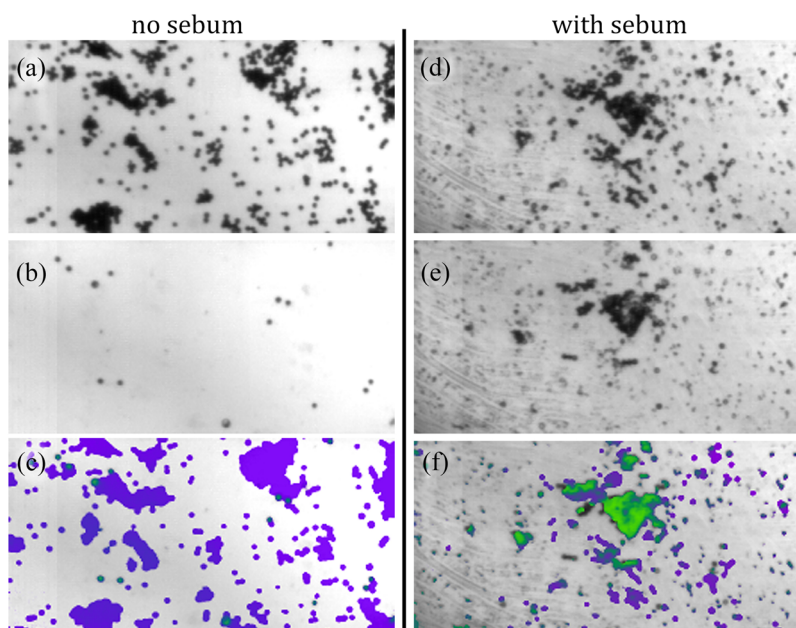

no sebum

with sebum

FIG. 3. Air jet impingement examples of 39 μm PSL removal from a glass slide. Left column: dry-deposited PSLs, (a) before jet impingement, (b) after jet impingement, (c) processed overlay—purple represents particles that have been removed, and green represents particles that remain on the surface after jet impingement. Right column: PSLs embedded in sebaceous fingerprint material, (d) before jet impingement, (e) after jet impingement, and (f) processed overlay. The video playback rate of the sebum example has been increased by 50× compared to dry deposit. Multimedia views: Left: https://doi.org/10.1063/1.5096488.6; Right: https://doi.org/10.1063/1.5096488.7

These examples provide spatially and temporally resolved images of particle removal. The time scales of these two examples are quite different—the dry-PSL event is very fast, with almost all PSLs removed in about 10 ms. The sebum-PSL event lasts almost 500 ms. To remove particles with increased adhesion, jet pulse duration should be lengthened, or multiple pulses should be used.

Aerodynamic removal of microparticles from surfaces has been the focus of many research efforts.[10,27,28] This new imaging tool combines existing counting methods with a robust *in situ* visualization tool that can uncover the mechanisms of individual particle detachment, not just before and after counting. Using this system along with image processing, it is possible to study the velocity of the particles, the time delay from jet pulse until the onset of particle motion, the particle acceleration, and the qualitative mode of particle removal.

CONCLUSIONS

In conclusion, a unique imaging system has been developed that leverages high-speed microvideography with microparticle sampling visualization. This system is used to study the dynamic interparticle and surface-particle events that occur when a wipe material is translated across a contaminated glass slide. Additionally, the same system can be used to study aerodynamic particle sampling providing insights into air jet impingement dynamics and mechanisms of particle removal. We view this instrument as an innovative tool that will support efforts to improve trace particle sampling methodologies and help in the development of next-generation sampling materials and methods.

One limitation of the current instrument is that the sampling substrate must be glass or some other transparent material. While glass is not always the most relevant surface for trace contraband detection, it has served for decades as a model surface for studying particle removal mechanisms via wipe sampling and aerodynamic sampling.[28–32] Additionally, we have not specifically addressed whether particles are sliding or rolling along the surface. However, there is a possibility that new image processing techniques could be used to determine the particle motion during wipe sampling.[33] With this added feature, one could begin to visualize the underlying mechanisms of particle removal in both wipe sampling and noncontact aerodynamic sampling activities.

Certain commercial products are identified in order to adequately specify the procedure; this does not imply endorsement or recommendation by NIST nor does it imply that such products are necessarily the best available for the purpose.

ACKNOWLEDGMENTS

REFERENCES

[1] J. C. Patrick and E. J. Poziomek, in *Proceedings of Enabling Technologies for Law Enforcement and Security* (SPIE, 1997).

[2] N. I. o. Justice, Annual Report 602-00, 2003.

[3] F. Li, Z. Xie, H. Schmidt, S. Sielemann, and J. I. Baumbach, Spectrochim. Acta, Part B **57**, 1563 (2002).

[4] G. A. Eiceman and J. A. Stone, Anal. Chem. **76**, 390A (2004).

[5] N. R. Council, *Assessment of Technologies Deployed to Improve Aviation Security: First Report* (The National Academies Press, Washington, DC, 1999).

[6] D. Shea and P. E. Morgan, CRS Report for Congress, 2005.

[7] G. A. Eiceman, TrAC, Trends Anal. Chem. **21**, 259 (2002).

[8] H. Gowadia and G. Settles, J. Forensic Sci. **46**, 1324 (2001).

[9] G. S. Settles, Annu. Rev. Fluid Mech. **38**, 87 (2006).

[10] D. Phares, J. Holt, G. Smedley, and R. Flagan, J. Forensic Sci. **45**, 774 (2000).

[11] G. S. Settles, J. Fluids Eng. **127**, 189 (2005).

[12] M. E. Staymates, W. A. MacCrehan, J. L. Staymates, R. R. Kunz, T. Mendum, T.-H. Ong, G. Geurtsen, G. J. Gillen, and B. A. Craven, Sci. Rep. **6**, 36876 (2016).

[13] B. A. Craven, M. J. Hargather, J. A. Volpe, S. P. Frymire, and G. S. Settles, IEEE Sens. J. **14**, 1852 (2014).

[14] G. S. Settles, in Proceedings of 2nd FAA Symposium on Explosives Detection and Aviation Security Technology, 1996.

[15] M. Staymates, G. Gillen, J. Grandner, and S. Lukow, in *Proceedings of 2011 IEEE International Conference on Technologies for Homeland Security (HST)* (IEEE, 2011).

[16] C. P. Lichtenwalner, Am. Ind. Hyg. Assoc. J. **53**, 657 (1992).

[17] J. R. Verkouteren, N. W. M. Ritchie, and G. Gillen Environ. Sci.: Processes Impacts **15**, 373 (2013).

[18] A. Dufresne, T. Mocanu, S. Viau, G. Perrault, and C. Dion, J. Environ. Monit. **13**, 74 (2011).

[19] J. L. Staymates, J. Grandner, and G. Gillen, Anal. Methods **3**, 2056 (2011).

[20] W. Chouyyok, J. T. Bays, A. A. Gerasimenko, A. D. Cinson, R. G. Ewing, D. A. Atkinson, and R. S. Addleman, RSC Adv. **6**, 94476 (2016).

[21] J. L. Staymates, M. E. Staymates, and J. Lawrence, Int. J. Ion Mobility Spectrom. **19**, 41 (2016).

[22] D. Fisher, R. Zach, Y. Matana, P. Elia, S. Shustack, Y. Sharon, and Y. Zeiri, Talanta **174**, 92 (2017).

[23] M. E. Staymates, J. Grandner, and J. R. Verkouteren, IEEE Sens. J. **13**, 4844 (2013).

[24] J. R. Verkouteren, J. A. Lawrence, M. E. Staymates, and E. Sisco, J. Visualized Exp. **122**, 55484 (2017).

[25] M. Sweat, A. Parker, and S. Beaudoin, Propellants, Explos., and Pyrotech. **41**, 855 (2016).

[26] J. R. Verkouteren, J. L. Coleman, R. A. Fletcher, W. J. Smith, G. A. Klouda, and G. Gillen, Meas. Sci. Technol. **19**, 115101 (2008).

[27] R. Fletcher, N. Briggs, E. Ferguson, and G. Gillen, Aerosol Sci. Technol. **42**, 1052 (2008).

[28] R. Keedy, E. Dengler, P. Ariessohn, I. Novosselov, and A. Aliseda, Aerosol Sci. Technol. **46**, 148 (2012).

[29] D. J. Phares, G. T. Smedley, and R. C. Flagan, J. Aerosol Sci. **31**, 1335 (2000).

[30] G. T. Smedley, D. J. Phares, and R. C. Flagan, Exp. Fluids **26**, 324 (1999).

[31] G. Ziskind, L. P. Yarin, S. Peles, and C. Gutfinger, Aerosol Sci. Technol. **36**, 652 (2002).

[32] M. Staymates, G. Gillen, W. Smith, R. Lareau, and R. Fletcher, in *Proceedings of the ASME Fluids Engineering Division Summer Conference* (ASME, 2010), Vol. 2.

[33] J. R. Agudo, G. Luzi, J. Han, M. Hwang, J. Lee, and A. Wierschem, Rev. Sci. Instrum. **88**, 051805 (2017).